Cerebral Cortex, November 2021;31: 4916–4932

https://doi.org/10.1093/cercor/bhab131
Advance Access Publication Date: 21 July 2021
Original Article

ORIGINAL ARTICLE

Symptom-Related Differential Neuroimaging Biomarkers in Children with Corpus Callosum Abnormalities

Yurui Guo[1,†], Alpen Ortug[1,†], Rodney Sadberry[1,2], Arthur Rezayev[1,3], Jacob Levman[1,4], Tadashi Shiohama[1,5] and Emi Takahashi[1]

[1]Division of Newborn Medicine, Boston Children's Hospital, Harvard Medical School, Boston, MA 02115, USA, [2]Department of Behavioral Neuroscience, Northeastern University, Boston, MA 02215, USA, [3]Department of Biology, Boston University, Boston, MA 02215, USA, [4]Department of Mathematics, Statistics and Computer Science, St. Francis Xavier University, Antigonish, NS B2G 2W5, Canada and [5]Department of Pediatrics, Chiba University Hospital, Chiba 2608670, Japan

Address correspondence to Emi Takahashi, Boston Children's Hospital, 300 Longwood Avenue, Boston, MA 02115, USA.
Email: emi@nmr.mgh.harvard.edu
[†]Yurui Guo and Alpen Ortug shared co-first authorship.

Abstract

We aimed to identify symptom-related neuroimaging biomarkers for patients with dysgenesis of the corpus callosum (dCC) by summarizing neurological symptoms reported in clinical evaluations and correlating them with retrospectively collected structural/diffusion brain magnetic resonance imaging (MRI) measures from 39 patients/controls (mean age 8.08 ± 3.98). Most symptoms/disorders studied were associated with CC abnormalities. Total brain (TB) volume was related to language, cognition, muscle tone, and metabolic/endocrine abnormalities. Although white matter (WM) volume was not related to symptoms studied, gray matter (GM) volume was related to cognitive, behavioral, and metabolic/endocrine disorders. Right hemisphere (RH) cortical thickness (CT) was linked to language abnormalities, while left hemisphere (LH) CT was linked to epilepsy. While RH gyrification index (GI) was not related to any symptoms studied, LH GI was uniquely related to cognitive disorders. Between patients and controls, GM volume and LH/RH CT were significantly greater in dCC patients, while WM volume and LH/RH GI were significantly greater in controls. TB volume and diffusion indices for tissue microstructures did not show differences between the groups. In summary, our brain MRI-based measures successfully revealed differential links to many symptoms. Specifically, LH GI abnormality can be a predictor for dCC patients, which is uniquely associated with the patients' symptom. In addition, patients with CC abnormalities had normal TB volume and overall tissue microstructures, with potentially deteriorated mechanisms to expand/fold the brain, indicated by GI.

Key words: agenesis of corpus callosum, cognitive outcome, corpus callosum, epilepsy

Introduction

The corpus callosum (CC) is the largest commissural tract of the human brain responsible for the transmission of motor, sensory, and cognitive information between the two hemispheres (Rotmensch and Monteagudo 2020). Descriptions of the CC abnormalities include dysgenesis of the CC (dCC) defining inadequate formation or abnormal shape of the CC; agenesis of the CC (AgCC), in which the structure is partly or completely missing; and hypoplasia of the CC (hCC) as defining decreased CC thickness (Sauerwein et al. 1981; Mooshagian et al. 2009; Edwards et al. 2014; Rotmensch and Monteagudo 2020; Vasung

© The Author(s) 2021. Published by Oxford University Press. All rights reserved. For permissions, please e-mail: journals.permissions@oup.com

et al. 2020). However, there is confusion and variability about the use of the terms partial AgCC and hCC in the literature (Schell-Apacik et al. 2008). For example, while some studies considered that partial AgCC and hCC under a definition of dCC as its subgroups (e.g. Palmer 2014), other studies defined complete and partial AgCC as the subgroups of dCC, and hCC as a different group (e.g. Vasung et. al. 2020), and others considered dCC as an umbrella term including both partial/complete AgCC and hCC (Tovar-Moll et al. 2004, Bénézit et al. 2015). As such, the choice of the terminology of the descriptions of CC abnormalities in the literature varies and is often confusing in this research field. Since dCC can be used as a general terminology for any malformation of the CC (Tovar-Moll et.al 2004, Bénézit et al. 2015), we chose to follow their suggestions, using dCC as an umbrella term including two subgroups: partial/complete agenesis of the CC (subgroup Absence) and decreased thickness of the CC (subgroup Hypoplasia).

The etiology of the CC abnormalities may be a result of a variety of different genetic or environmental factors during the fetal period (Yuan et al. 2020). Recent research suggests that multiple genetic mechanisms, including single-gene Mendelian mutations, single-gene random mutations, and complex genetics, may be effective (Paul et al. 2007). It is reported that approximately 55–70% of the cases are not clinically identifiable. Some cases are associated with external stimuli such as alcohol consumption in pregnancy (Edwards et al. 2014). Additionally, dCC is a feature of Aicardi's syndrome and is presumed to be caused by an X-linked dominant *de novo* mutation that is lethal in males in which no candidate genes have been identified (Kroner et al. 2008).

The prevalence of the dCC varies in the literature ranging from 0.5 per 10 000 in the general population to 230–600 per 10 000 in children with neurodevelopmental disability (Palmer and Mowat 2014). This difference may be the result of ambiguity in the definition of the type of callosal abnormalities between studies and their varied results (Palmer and Mowat 2014). Developmental milestones such as walking, talking, and reading are typically delayed to varying extent in children with dCC. Motor skills, especially those involving left–right coordination, may be a particular challenge. Patients with dCC have a broad range of clinical deficits; many have symptoms that fall within the autistic spectrum (Badaruddin et al. 2007) and suffer from seizures and spastic episodes (Heimer et al. 2015). In some cases, dCC patients show mental retardation, mostly with mildly impaired intelligence or subtle psychosocial symptoms. Although partial/complete AgCC is frequently accompanied by malformations of the cerebral cortex, it also appears as an isolated neuroradiological finding. Therefore, isolated AgCC (dCC) is of interest to both the clinical communities and researchers, as the neurological and psychological symptoms of these patients vary from discrete to life disabling.

The goals of our work were to identify neurological symptoms and neuroimaging biomarkers in patients with CC abnormalities. We correlated quantitative and qualitative magnetic resonance imaging (MRI) measures in patients with dCC with the retrospectively retrieved clinical outcome to identify what types of quantitative neuroimaging measures could be biomarkers of patients with CC abnormalities. We hypothesized that there were specific brain MRI-based measures that could characterize regional brain abnormalities outside of the CC in patients with CC abnormalities, and some of them would be linked to symptoms of the patients.

Materials and Methods

Subjects

We retrieved radiological reports from the Boston Children's Hospital (BCH) radiological database using the following keywords: agenesis, dysgenesis, hypogenesis, hypoplasia, and thinning of the CC (Figure 1). The search yielded 87 patients with CC disorders ($N = 66$ with isolated CC disorder, $N = 21$ with CC disorders, and an associated cortical malformation). MRI data and neurological reports of these patients were retrospectively used. A normal age- and sex-matched control group was also assembled using the BCH patient database. Since the study was retrospective in nature, and no identifying information was requested by the researchers, it was determined that informed consent would not be sought from the patients due to the low risk it presented to them. A waiver of patient consent, in addition to all other procedures, was approved after due consideration by the BCH Institutional Review board.

MRI Scan Parameters

Participants were imaged with clinical 3 Tesla MRI scanners (Skyra, Siemens Medical Systems, Erlangen, Germany) at BCH yielding T1-weighted structural volumetric images accessed through the Children's Research and Integration System (Pienaar et al. 2015). Spatial resolution ranged from $0.49 \times 0.49 \times 1$ mm^3 to $1.15 \times 1.15 \times 1$ mm^3. Diffusion MRI data were typically acquired using isotropic diffusion-weighted spin-echo echo-planar imaging with repetition time (TR) = 10 s; echo time (TE) = 88 ms; $\delta = 12.0$ ms; $\Delta = 24.2$ ms; matrix size = 128×128; integrated parallel imaging techniques (iPAT) = 2; and five b0 and 30 diffusion-weighted measures with the high b value of 1000 s/mm^2. Spatial resolution varied in the x and y directions from 1.57 to 2.10 mm (mean: 1.76 mm, standard deviation [SD]: 0.11 mm). Through-plane slice thickness varied from 2.00 to 2.60 mm (mean: 2.10 mm, SD: 0.19 mm).

T1w MRI Quality Control and Processing

A diagram of inclusion/exclusion and control of the patients are shown in Figure 1. The criteria for MRI quality control were only based on the quality of scans, and it was not related to demographic factors such as gender, age, and diagnosis. Thus, MRI images with severe movements, poor white matter (WM) to gray matter (GM) contrast, severe hydrocephalus, artifacts, or shape distortions were excluded. Quality control of T1-weighted MRIs resulted in subdivision of patients into four groups: excellent ($N = 20$), very good ($N = 22$), satisfactory ($N = 18$), and poor T1w quality ($N = 25$), among which there were severe movement in 52%, poor WM to GM contrast in 28%, and severe hydrocephalus, artifacts, or shape distortions in 20% of cases. Only the patients with excellent, very good, or satisfactory T1-weighted MRI quality were included in further analysis ($N = 60$).

T1w MRI images were processed using the CIVET 2.1.0 pipeline (http://www.bic.mni.mcgill.ca/ServicesSoftware/CIVET), designed for extraction of cortical surfaces and calculation of cortical thickness (CT). We performed the following processes:

1. Linear registration of original MR images to the standardized MNI space (ICBM 152 dataset) (Fonov et al. 2009).
2. Tissue segmentation of MR images into the cerebrospinal fluid and GM and WM, with partial volume estimates of the tissue classes (Zijdenbos et al. 1998; Tohka et al. 2004).

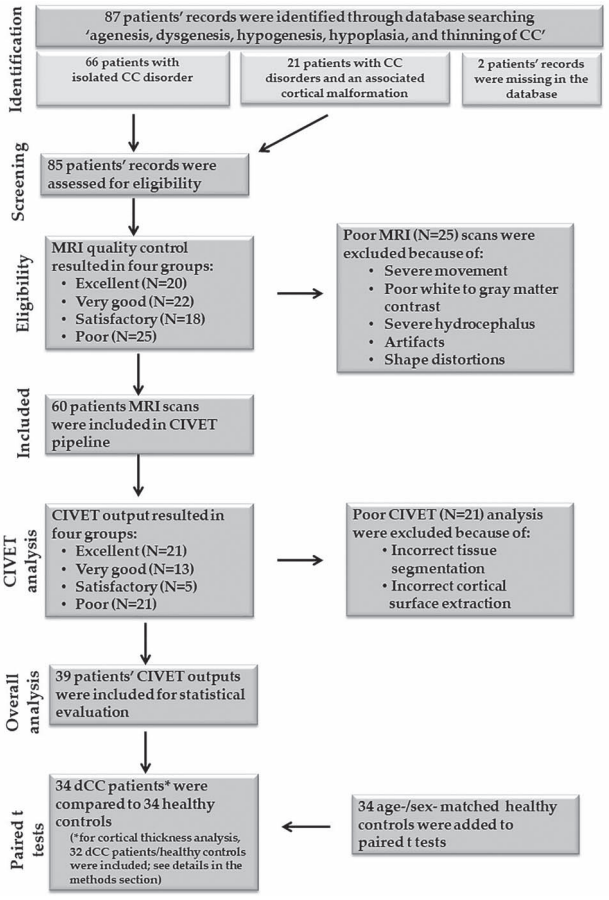

Figure 1. Flow diagram for inclusion, exclusion, overall analysis, and statistics.

3. Correction of the intensity of nonuniform artifacts, using the N3 method (Sled et al. 1998), one of the crucial steps in T1-weighted MRI analysis since nonhomogeneity of the magnetic field leads to nonuniformity of MR intensity in the GM and WM.
4. Fully automatic extraction of the pial (outer cortical) and GM/WM boundary (inner cortical) surfaces (MacDonald et al. 2000; Kim et al. 2005) based on the segmented images. Surfaces were extracted by hemisphere by fitting the segmented images with a deformable mesh model with 163 840 triangles per hemisphere. In this step, 81 920 vertices (cortical points) were placed on the inner and outer cortical surfaces for each hemisphere of each subject.
5. Registration of the mid-cortical surface of each subject to an average surface template (ICBM 152 data set) (Robbins 2004; Lyttelton et al. 2007; Boucher et al. 2009) to establish the inter-subject correspondence of surface vertices.

After the quality control of the CIVET output files, hand-drawn masks of ventricles were created in Display (http://www.bic.mni.mcgill.ca/software/Display/Display.html) to correct segmentation errors. Corrected segmentations of the ventricles were imported back into the CIVET pipeline to improve the quality of the segmentation and extraction of cortical surfaces. The CIVET pipeline was re-run using newly created masks until satisfactory CIVET output was obtained. Such a step was necessary due to the large anatomical differences in the dCC population studied.

The final quality check of the CIVET output files was performed to ensure accurate tissue segmentation and cortical surface extraction. From 60 patients, 39 patients who had excellent ($N = 21$), very good ($N = 13$), or satisfactory ($N = 5$) CIVET output (65%) were included in the further analyses (mean age 8.08 ± 3.98).

The total brain (TB) volume and the volume of the cerebral cortex, WM, and ventricles were calculated by summing the volumes of all the voxels belonging to tissue classes. The TB volume included only the cerebral and cerebellar tissues (GM and WM) excluding the cerebrospinal fluid. The gyrification index (GI) was calculated by dividing the area of each cortical surface by the corresponding area of its convex hull, for each hemisphere.

In addition, three brain abnormalities (CC, GM, and brain size abnormalities) were reported categorically as several abnormal groups according to the degrees. The abnormality of brain size was inspected and reported by a radiologist or a physician, and head circumference and growth curve measures were a part of the clinical review. GM abnormalities such as GM heterotopia, gyrification abnormality or encephalopathies, and different types of callosal abnormalities were also included in the clinical reviews.

Finally, the dCC patients were grouped into two subgroups: Absence ($N = 18$) and Hypoplasia ($N = 21$) (Fig. 2). Normal age- and sex-matched controls ($N = 39$), with excellent quality of T1-weighted MRIs and without evidence of brain pathology, were selected from the BCH radiological database and processed with the same version of CIVET using the CBRAIN portal (Sherif et al. 2014). The CBRAIN portal was used for controls, as manual corrections of the segmentation were not needed for controls. Of the 39 controls, 34 had an excellent or satisfactory CIVET output and were included in further quantitative MRI analyses. In all included subjects, the mid-sagittal area of the CC was manually delineated and measured using OsiriX (https://www.osirix-viewer.com).

Diffusion MRI Quality Control and Processing

From the 87 patients with CC abnormalities initially selected, 69 patients (79%) had diffusion MRI data, or diffusion MRI data with satisfactory quality (e.g., without severe motion artifacts or distortions). However, only the subjects that had both diffusion MRI and satisfactory or excellent CIVET output were included in further quantitative diffusion analysis ($N = 49$: dCC = 27, controls = 22). Of the 49 subjects whose diffusion data were included in the final analyses, 44 subjects had diffusion MRI with 35 measurements (five b0 volumes along with 30 volumes with a high-b value of 1000 s/mm^2). For those subjects, cortical masks were obtained from the CIVET pipeline. All diffusion MRI data were corrected for eddy current and motion using FSL (https://fsl.fmrib.ox.ac.uk/fsl). T1-weighted MRIs and the cortical masks for each of these patients were linearly co-registered with their b0 images (Supplementary Fig. S1).

Fractional anisotropy (FA) and apparent diffusion coefficient (ADC) values were calculated with a standard diffusion tensor model using Diffusion Toolkit (http://www.trackvis.org/). Brain mask volumes created by Diffusion Toolkit were used to terminate tractography instead of using the standard FA threshold (Schmahmann et al. 2007; Wedeen et al. 2008; Takahashi et al. 2010, 2011, 2012, 2014; Song et al. 2015; Vasung

Figure 2. CC disorders: abnormal shape of the CC (*A*), hypoplasia of the CC (*B*), absence of rostrum (*C*), genu and splenium (*D*), body (*E*), and body and splenium (*F*) of the CC. The complete absence of the CC is shown in (*G*).

et al. 2019), because progressive myelination and crossing fibers within the developing brain can result in low FA values, which may potentially incorrectly terminate tractography in brain regions with low FA values (Wilkinson et al., 2017). Mean FA and ADC measurements of the entire cerebral cortex were calculated using TrackVis (http://www.trackvis.org/) by superimposing linearly registered cortical masks on the FA (or ADC) maps.

Statistical Analyses

To analyze the correlation between brain MRI findings (brain abnormalities/brain measurements) and clinical/cognitive characteristics, data from a total of 78 participants (39 dCC patients and 39 controls) were used as input to the multiple logistic regressions of three radiologically reported brain abnormalities (CC, GM and brain size abnormalities) versus clinical/cognitive characteristics, and data from a total of 71 participants (39 dCC patients and 32 controls) were used as input to the multiple logistic regressions of MRI brain measurements (TB volume, cortical GM volume, GI in left hemisphere [LH]/right hemisphere [RH], CT in LH/RH) versus clinical/cognitive characteristics. Age and gender were also included in every model to take their influences on clinical symptoms into account.

Chi-squared tests and *t*-tests were performed for comparisons of age, gender, CC area, and brain abnormalities within the dCC patient group (between two subgroups: Hypoplasia $N = 21$, Absence $N = 18$). Paired *t*-tests were performed for comparisons of MRI brain measurements and clinical/cognitive characteristics between the Hypoplasia subgroup (18 patient and control pairs)/the Absence subgroup (15 patient and control pairs) and their controls.

Analyses between dCC patient and control groups were conducted by performing paired *t*-tests. Comparisons included MRI brain measurements and cortical DTI measurements: TB volume (34 patient and control pairs), cortical GM volume (34 patient and control pairs), WM volume (34 patient and control pairs), GI in LH/RH (34 patient and control pairs), CT (32 patient and control pairs) in LH/RH, FA of the cerebral cortex (16 patient and control pairs), and ADC of the cerebral cortex (16 patient and control pairs). In this set of tests, the volumes of GM and WM were both normalized by the TB volumes, after which, therefore, the normalized values of GM and WM were percentages of TB volumes.

Paired *t*-tests need gender-/age-matched patient and control pairs, and the differences of age in every patient and control pair were from 0.002 to 0.081 years old. However, not each patient had a corresponding control, so after pairing, the numbers of patient and control pairs varied in each test.

The confidence level for all tests was 95%, and the Bonferroni correction was applied.

Statistical analyses (descriptive, tests) were performed using SPSS (https://www.ibm.com/analytics/spss-statistics-software) software and RStudio (https://www.rstudio.com/).

Results

Demographical and Radiological Characteristics of Patients with CC Disorders

Of the 39 patients with CC abnormalities, 48.7% were males and 51.3% females. The mean age at the MR scan was 8.08 years with an SD of 3.98 years. Almost half of the patients had hypoplastic CC (53.8%), while the rest of them had a partial or total absence of CC (46.2%). The most frequent disorder of CC was the total hypoplasia (35.9%) and complete AgCC (20.5%). Almost 36% of patients (35.9%) had an additional abnormality of GM. Similarly, 31% of patients had an abnormality in brain size. Detailed demographical and radiological characteristics of the patient group were reported in Table 1. Additionally, a detailed classification of brain abnormalities was presented within a Venn diagram (Fig. 3). Distributions and overlapping of GM abnormality and brain size abnormality in dCC patient group ($N = 39$), dCC subgroup Hypoplasia ($N = 21$), and subgroup Absence ($N = 18$) were shown.

Genetic, Clinical, and Cognitive Characteristics of Patients with Callosal Abnormalities

Out of 39 patients, 36 had one or more neurological symptoms (see Table 2). Fourteen patients had epilepsy, while one had an epileptic activity on EEG, indicating a predisposition to generate seizures. The most frequent neurological disorder was language impairment ($N = 25$). Out of 25 patients with language impairment, 5 patients were averbal, 1 patient had only a receptive language disorder, 8 patients had an expressive language disorder, while 11 patients had both expressive and receptive language disorders. The second most frequent neurological disorder was cognitive disorder ($N = 24$) such as global or mild developmental delay, intellectual disabilities, mild learning disabilities, communication problems, and unspecific neurodevelopmental disorders. The most frequent among those were global developmental delay ($N = 15$), followed by intellectual disability ($N = 4$), unspecific neurodevelopmental disorder ($N = 2$), mild developmental delay ($N = 1$), mild learning disabilities ($N = 1$), and communication impairment ($N = 1$).

Following the language and cognitive disorders, there were muscle tone abnormalities (hypotonia [$N = 12$] or hypertonia [$N = 9$]), abnormalities of motor skills/movement (impairments of fine motor skills [$N = 8$], gross motor skills [$N = 5$], and dyskinesia [$N = 5$]), and eye or ocular motor abnormalities (strabismus [$N = 5$], amblyopia [$N = 3$], astigmatism [$N = 2$],

Table 1 Patient characteristics, patient age during MRI scan, and MRI findings additional to abnormality of the CC

	N/Value	Percentage
Total number	39	
Male	19	48.7%
Female	20	51.3%
Age during MRI scan (years)		
Mean (±SD)	8.08 (±3.98)	
CC abnormality		
1) Hypoplastic CC	21	53.8%
Middle segment hypoplasia	4	10.3%
Posterior segment hypoplasia	3	7.7%
Hypoplasia of all segments	14	35.9%
2) Absence of CC	18	46.2%
Absence of the rostrum	1	2.6%
Middle segment absence	1	2.6%
Posterior segment absence	5	12.8%
Near absence	3	7.7%
Complete agenesis	8	20.5%
GM abnormality	14	35.9%
Ectopic GM	5	12.8%
Gyrification abnormalities	5	12.8%
Combined	2	5.1%
GM injury (encephalopathy)	2	5.1%
Abnormalities of brain size	12	30.8%
Microcephaly	8	20.5%
Macrocephaly	3	7.7%
Holoprosencephaly	1	2.6%

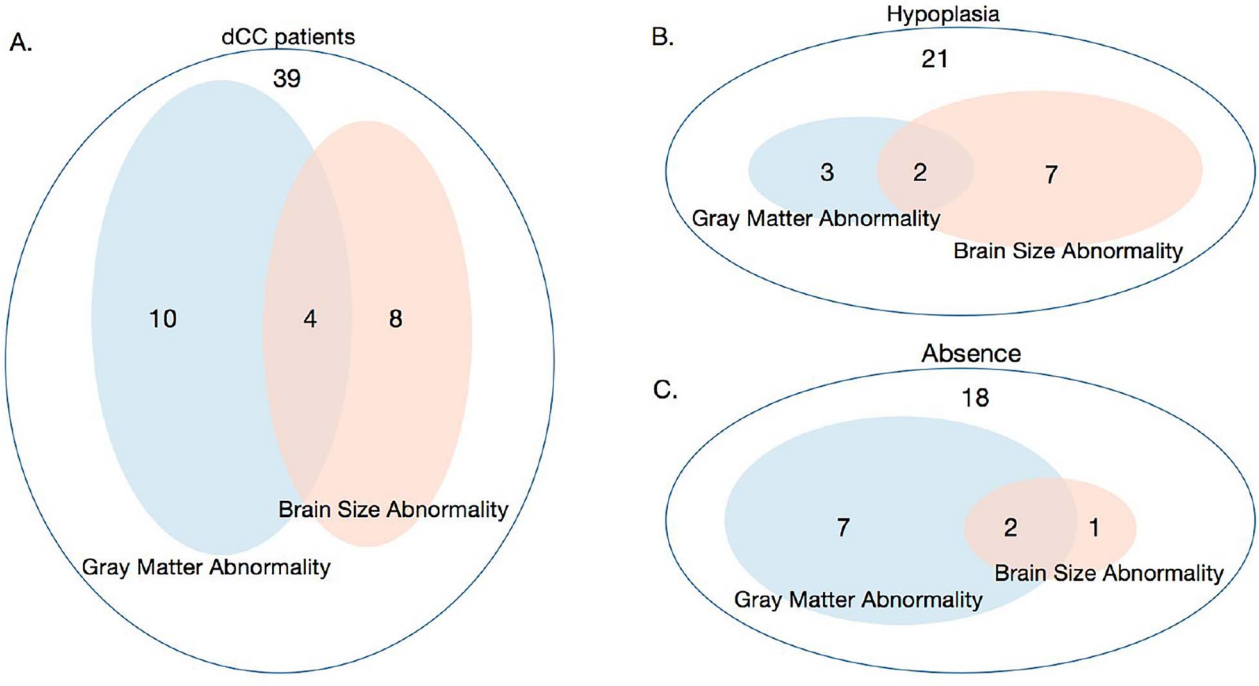

Figure 3. Venn diagram showing detailed classifications of brain abnormalities in all dCC patients (A), subgroup Hypoplasia (B), and subgroup Absence (C).

heterophoria [$N = 1$], septo-optic dysplasia [$N = 1$], eccentric pupil [$N = 1$], difficulty with voluntary abduction [$N = 1$], and pathophysiologic saccades [$N = 1$]).

Sixteen patients had behavioral disorders such as attention deficit hyperactivity disorder ($N = 7$); delayed social skills development, pervasive developmental disorder, or autism

Table 2 Genetic, clinical, and cognitive characteristics of patients with dCC

	N	Percentage
Neurological		
Eye or ocular motor abnormalities	15	38.5%
Hearing abnormalities	5	12.8%
Muscle tone abnormalities	21	53.8%
Abnormalities of motor skills/movement	18	46.2%
Language impairment	25	64.1%
Cognitive disorder	24	61.5%
Behavioral disorder	16	41.0%
Sleep disorder	7	17.9%
Epilepsy	15	38.5%
Metabolic or endocrine disorder	17	43.6%
Genetic disorder	13	33.3%

($N = 5$); self-injurious behavior ($N = 2$); episodic mood swings ($N = 1$); and disruptive behavior disorder ($N = 1$).

Almost half of the patients ($N = 17$) had metabolic disorder (propionic academia [$N = 1$], absence of CYP2C9 [$N = 1$], blood lactate and pyruvate levels with or without lactic acidemia [$N = 1$], hyperammonemia [$N = 1$], uncoupling of oxidative phosphorylation [$N = 1$], diabetes [$N = 1$], and leukodystrophy [$N = 1$]) or endocrine disorder (endocrine abnormalities associated with Koolen Vries syndrome [$N = 1$], premature adrenarche [$N = 2$], panhypopituitarism [$N = 1$], hypothalamic obesity [$N = 1$], hypergonadotropic hypogonadism [$N = 1$], endocrine disorder associated with CHARGE syndrome [$N = 1$], hypothyroidism [$N = 2$], and Helsmoortel-van der Aa Syndrome [$N = 1$]).

One third of patients ($N = 13$) had an identified genetic disorder. The most frequently identified genetic disorder was a single gene (CDKL5 mutation on X chromosome [$N = 1$], BRAF mutation [$N = 1$], KANSL1 gene mutation [$N = 1$], and de novo mutation of ADNP gene [$N = 1$]) or chromosomal mutation (Turner syndrome [$N = 1$], partial trisomy 18 [$N = 1$], ring chromosome 8 [$N = 1$], and trisomy 17p [$N = 1$]). The rest of the patients with genetic disorder had identified gene deletion (1q42.12-q42.2 deletion [$N = 1$]), gene deletion with a duplication (MECP2 deletion and chromosome 8 duplication [$N = 1$]), translocation (translocation between 4p16 and 15p13, deletion of 1p21.1 [$N = 1$]), or mutation (copy number variants, 6p13.3 max 215 KB deletion, 22q11.21 max 583 KB gain [$N = 1$]).

A detailed classification of the symptoms was given in a pie chart (Fig. 4). Symptoms and disorders had different proportions in isolated dCC patients and dCC with additional brain abnormalities.

Correlations between Brain MRI Findings and Clinical/Cognitive Characteristics

The analysis results between cortical/connectivity anomalies and symptoms were shown in Table 3. A symptom with statistical significance meant that it was related to that abnormality. The results indicated that except for hearing, cognitive, and sleeping disorders, most symptoms/disorders studied were associated with CC abnormalities. The abnormalities would increase the probability of suffering from muscle tone, motor skills/movements, language, metabolic/endocrine, and behavioral abnormalities. GM abnormalities included in all models did not show a significant effect. Brain size abnormalities were related to language and cognitive disorders, and it would increase the probability of suffering from these abnormalities.

Behavioral characterizations were based on neurological assessments, and parent reports often supported them. A variety of different assessment tests were used to assess the dCC patients. Denver developmental assessment, early intervention developmental profile assessment, and ski-hi language development scale were examples of developmental test that were applied. For mental status, a psychiatry/psychology consultation was requested, and the patients were evaluated according to the DSM-IV Multiaxial Diagnosis, and Clinical Global Impression, which reveals a Children's Global Assessment Scale. Our control patients were people admitted to the hospital having headache or other concerns but found no abnormalities after MRI evaluation and clinical examination so they were not able to receive the same assessments applied to patients with CC abnormalities.

To study whether and how brain MRI measurements are associated with those symptoms, multiple logistic regression models were built for each symptom based on MRI measurements (Table 4). TB volume was negatively related to language, cognition, muscle tone, and metabolic/endocrine abnormalities. Although WM volume was not related to any symptoms studied, GM volume was related to cognitive, behavioral, and metabolic/endocrine disorders. Larger GM volume may slightly increase the likelihood of having disorders in cognitive, behavioral, and metabolic/endocrine domains. RH CT had a positive correlation with language abnormalities, while LH CT had a positive correlation with epilepsy. LH and RH CT were both related to muscle tone abnormalities; however, the correlations were the opposite. A larger LH CT would increase the likelihood of having muscle tone abnormalities, while a larger CT in RH would decrease the likelihood of having such abnormalities. This may suggest that the larger the difference between CT in LH and RH (LH CT larger than RH CT), the higher the likelihood of having muscle tone abnormalities would be. In addition, while the RH gyrification index (GI: the ratio between contours of the folded and interpolated outer brain surfaces) was not related to any symptoms studied, LH GI was uniquely related to cognitive disorders. Larger LH GI may decrease the likelihood of suffering from cognition disorders. These results suggested that brain MRI-based measurements reveal differential effects to many symptoms associated with dCC.

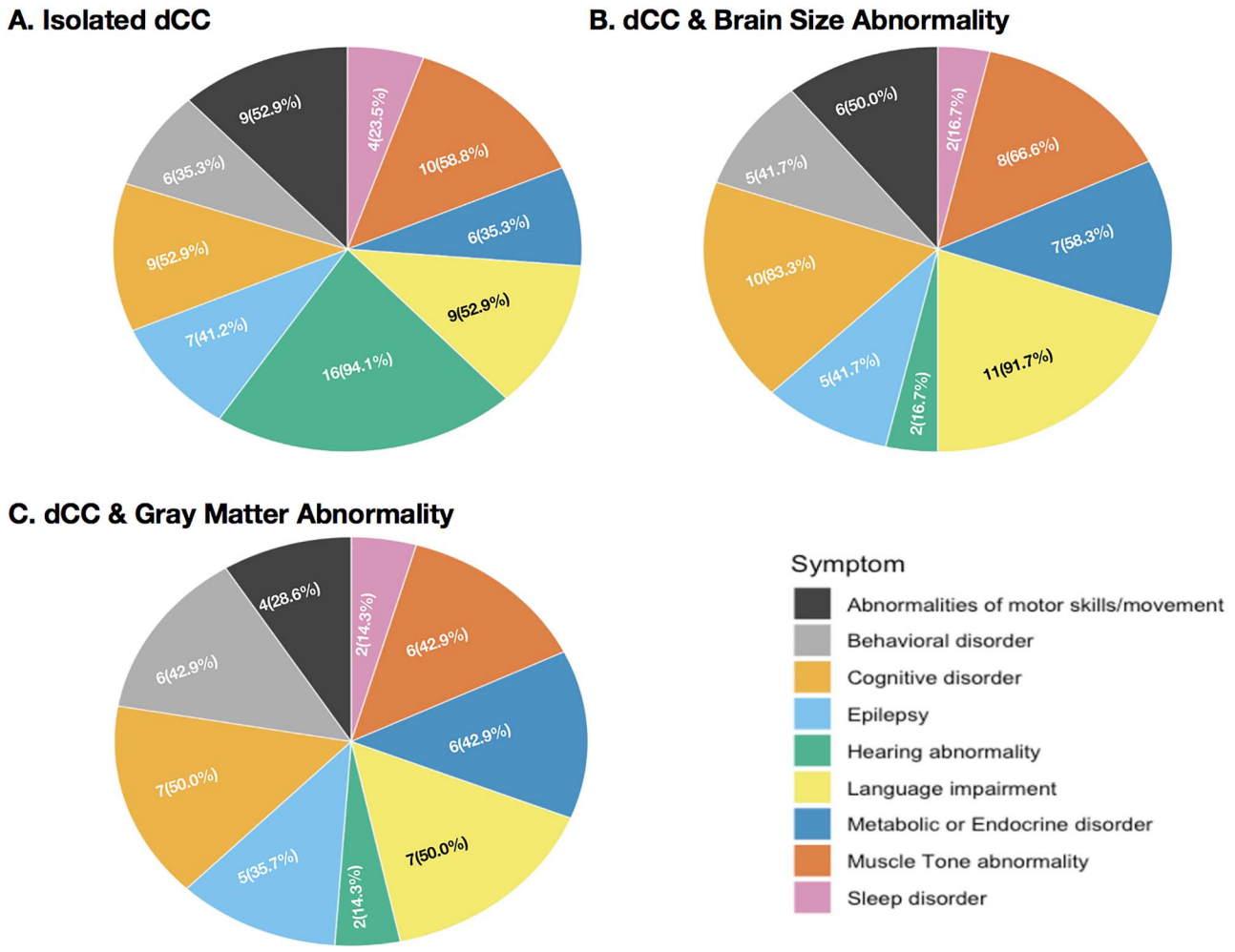

Figure 4. Pie chart showing detailed classifications of symptoms in isolated dCC group (A), dCC with Brain Size abnormalites group (B), and dCC with Gray Matter abnormalities group (C).

Within-Group Analysis

To ensure that patients with dCC represent a relatively homogenous group to compare to the control group, a set of tests (t-tests and chi-squared tests) was performed to compare the differences between the two subgroups (Hypoplasia and Absence), as well as each subgroup with their corresponding gender-/age-matched control groups. However, the results suggested that there was no significant difference between these two subgroups in patient characteristics, presence of neurological, endocrine/metabolic, brain, genetic abnormality, region of CC affected, or in quantitative brain measures including the CT (Table 5). In addition, in the CC Absence subgroup ($N = 18$), considering that the developmental mechanisms between CC total and partial absence might be different, we further compared MRI brain measurements and clinical symptoms 1) between patients with complete CC absence ($N = 8$) and patients with partial CC absence ($N = 10$), 2) between patients with complete CC absence and their age/sex-matched controls (7 pairs of patient & control), and 3) between patients with partial CC absence and their age/sex-matched controls (8 pairs of patient & control). All of these comparisons showed no statistically significant difference.

Between-Group Analysis

Figure 5 shows the ORs (log-scaled values) of disorders for dCC patients. OR, a measure of association between exposure and an outcome, in our case, was the ratio of the odds of having a disorder in the patients and the odds of having a disorder in the control group. An OR of 1 (log-scaled threshold = 0) indicates dCC not affecting on suffering from that disorder; OR > 1 (log-scaled threshold = 0) indicates increased occurrence of disorder in the presence of dCC; OR < 1 (log-scaled threshold = 0) indicates decreased occurrence of disorder in the presence of dCC.

Compared to the age- and sex-matched control group, patients with dCC had significantly higher odds of having GM abnormality (OR = 44.92, 95% CI [2.57, 786.66]), gene/chromosomal abnormality (OR = 9.2, 95% CI [1.92, 44.5]), endocrine or metabolic disorders (OR = 14.3, 95% CI [3.01, 67.84]), epilepsy (OR = 23.75, 95% CI [2.94, 191.57]), eye or ocular motor abnormalities (OR = 23.75, 95% CI [2.94, 191.59]), muscle tone abnormalities (OR = 44.33, 95% CI [5.52, 355.93]), motor skills/movement abnormalities (OR = 7.5, 95% CI [2.23, 25.18]), language impairment (OR = 67.86, 95% CI [8.39, 548.95]), cognitive disorder (OR = 124.88, 95% CI [7.14, 2182.53]), and behavioral disorder (OR = 8.35, 95% CI [2.19, 31.86]).

Table 3 Analysis of brain abnormalities with clinical and cognitive characteristics

Symptoms	Statistics	CC abnormalities	GM abnormalities	Brain size abnormalities
Hearing abnormalities	P value	0.741	0.634	0.518
	Estimate	0.329	0.502	0.680
	SE	0.993	1.054	1.052
	z value	0.331	0.476	0.646
Muscle tone abnormalities	P value	**6.580×10^{-4}**	0.403	0.268
	Estimate	3.800	−0.591	0.835
	SE	1.115	0.706	0.754
	z value	3.407	−0.837	1.108
Abnormalities of motor skills/movement	P value	**9.910×10^{-4}**	0.177	0.647
	Estimate	2.355	−0.993	0.343
	SE	0.715	0.736	0.748
	z value	3.293	−1.349	0.458
Language impairment	P value	**9.440×10^{-4}**	0.776	**0.027**
	Estimate	3.763	0.223	2.702
	SE	1.138	0.794	1.219
	z value	3.307	0.281	2.217
Metabolic or endocrine disorder	P value	**0.004**	0.757	0.316
	Estimate	2.618	−0.224	0.742
	SE	0.903	0.725	0.739
	z value	2.900	−0.309	1.004
Cognitive disorder	P value	0.994	0.196	**0.031**
	Estimate	2.102×10^{1}	−1.046	2.481
	SE	2.778×10^{4}	0.808	1.152
	z value	0.008	−1.294	2.154
Behavioral disorder	P value	**0.007**	0.834	0.909
	Estimate	2.059	0.145	0.081
	SE	0.765	0.695	0.715
	z value	2.693	0.209	0.114
Sleeping disorder	P value	0.395	0.537	0.822
	Estimate	0.649	−0.579	−0.213
	SE	0.763	0.939	0.946
	z value	0.850	−0.617	−0.225

Note: Significant *P* values are shown in bold. SE, standard error.
Statistics of multiple logistic regression models are shown. All models included gender and age, but statistics not included in table. Confidence level: 95%.

Between the dCC and control groups, GM/WM volumes and LH/RH GI were statistically significantly different, except for TB volume (Table 6, Fig. 6). Patients with dCC, compared to the controls, had statistically significantly larger volumes of the GM and had statistically significantly smaller volumes of the WM and GI of each hemisphere. The TB volume was not found to be significantly different between groups.

Although the patients with dCC had significantly thicker cortex compared to the controls (Fig. 7), we did not find significant differences in cortical ADC and FA between patients with dCC and controls (Table 7, Fig. 8).

Discussion

In this retrospective MRI study, we have assessed quantitative and qualitative MRI characteristics of the brain, along with clinical symptoms of the patients with callosal abnormalities. The majority (93%) of the patients with dCC had at least one neurological symptom affecting the cognitive, behavioral, sensory, or motor domain, and the severity of those symptoms varied from discrete to life disabling. In addition, patients with dCC who had genetic disorders showed heterogeneous profiles. Given the heterogeneous nature of the disorder, the identification of imaging biomarkers for dCC remains of importance for the clinical community. Our results together suggest that brain MRI-based measures successfully revealed differential links to many symptoms in patients with dCC. Therefore, the assessment of brain MRI in patients with dCC has great potential for the understanding of the structural basis that underlies heterogeneous clinical symptoms seen in dCC patients.

Clinical and Genetic Heterogeneity of the Disorder

The biological basis of dCC is complex because it involves numerous genetically regulated developmental processes (Gobius and Richards 2011). In addition, patients with dCC often have additional genetic abnormalities, structural abnormalities of the brain, and/or epilepsy (Paul et al. 2007), which were also observed in our study (Fig. 2, Table 2). The most frequently studied disorders of the CC, caused by the failure of callosal axons to cross the midline, can be easily identified by the presence of gross structural abnormalities in the mid-sagittal plane (Hetts et al. 2006; Paul et al. 2007; Edwards et al. 2014).

Table 4 Analysis of MRI measurements with clinical and cognitive characteristics

Symptoms	MRI measurements	*P* value	Estimate	SE	OR
Hearing abnormalities					
Muscle tone abnormalities	TB	**0.001**	−0.008	0.003	0.992
	CT LH	**0.018**	17.193	7.284	2.931×10^{7}
	CT RH	**0.046**	−14.663	7.345	4.283×10^{-7}
Abnormalities of motor skills/movement					
Language impairment	TB	**0.019**	−0.004	0.002	0.996
	CT RH	$\mathbf{1.380\times10^{-4}}$	3.286	0.862	26.747
Metabolic or endocrine disorder	TB	**0.004**	−0.009	0.003	0.991
	GM	**0.011**	0.016	0.006	1.106
Cognitive disorder	TB	**0.012**	−0.010	0.004	0.990
	GM	**0.014**	0.021	0.008	1.021
	GI LH	**0.002**	−10.362	3.368	3.161×10^{-5}
Behavioral disorder	GM	**0.007**	0.011	0.004	1.011
	CT LH	**0.008**	1.748	0.662	5.745
	CT RH	**0.008**	1.816	0.686	6.147
Sleeping disorder					
Epilepsy	CT LH	**0.006**	3.082	1.115	2.180×10^{1}

Note: Significant *P* values are shown in bold. Symptoms with blank in statistics referred to not having statistically significantly related MRI measurements according to the models. SE, standard error. Statistics of multiple logistic regression models were shown. All models included gender and age, but statistics not included in table. Confidence level: 95%.

Table 5 Within-group comparisons of patient characteristics, age during MRI scan, and MRI findings

	Hypoplasia	Absence	Test result*
Total (*N*)	21	18	$X^2(1) = 0.24$, $P = 0.62$
Male (%)	11 (52.4%)	8 (44.4%)	
Female (%)	10 (47.6%)	10 (55.6%)	
Patient age in years (mean ± SD)	9.01 ± 3.57	7 ± 4.25	$t(37) = 1.61$, $P = 0.12$
CC abnormality			
Area in mm^2 (mean ± SD)	357.96 ± 104.15	97.56 ± 123.21	$t(37) = 7.16$, $P < 0.01$
1) Hypoplastic/Absence of CC (%)	21 (100%)	18 (100%)	$X^2(2) = 4.37$, $P = 0.11$
Rostrum	0 (0%)	1 (5.6%)	
Mid-portion (%)	4 (19%)	1 (5.6%)	
Posterior (%)	3 (14.3%)	5 (27.8%)	
Near total (%)	0 (0%)	3 (16.7%)	
All segments (%)	14 (66.7%)	8 (44.4%)	
GM abnormality	5 (23.8%)	9 (50%)	$X^2(1) = 2.89$, $P = 0.09$
Ectopic GM (%)	0 (0%)	5 (27.8%)	
Gyrification abnormalities (%)	4 (19%)	1 (5.6%)	
Combined (%)	0	2 (11.1%)	
GM injury (encephalopathy) (%)	1 (4.8%)	1 (5.6%)	
Abnormalities of brain size	9 (42.9%)	3 (16.7%)	$X^2(1) = 3.12$, $P = 0.08$
Microcephaly (%)	6 (28.6%)	2 (11.1%)	
Macrocephaly (%)	2 (9.5%)	1 (5.6%)	
Holoprosencephaly (%)	1 (4.8%)	0	

Note: * Results of chi-squared and *t*-tests were provided. Confidence level: 95%.

However, the presence and severity of these abnormalities do not seem to correlate with the severity of clinical symptoms (Goodyear et al. 2001; Shevell 2002; Moutard et al. 2003). Almost 93% of the patients with dCC included in our study had at least one clinical symptom. This agrees with the study by Moutard et al. (2003), which reported that individuals with asymptomatic dCC are rare. Therefore, it is important to study in detail the functional impairments in these patients. In addition, given that severity of symptoms does not correlate with the mid-sagittal malformation, it is important to find improved neuroimaging tools with the ability to detect subtle abnormalities such as GM/WM volume, CT, and GI.

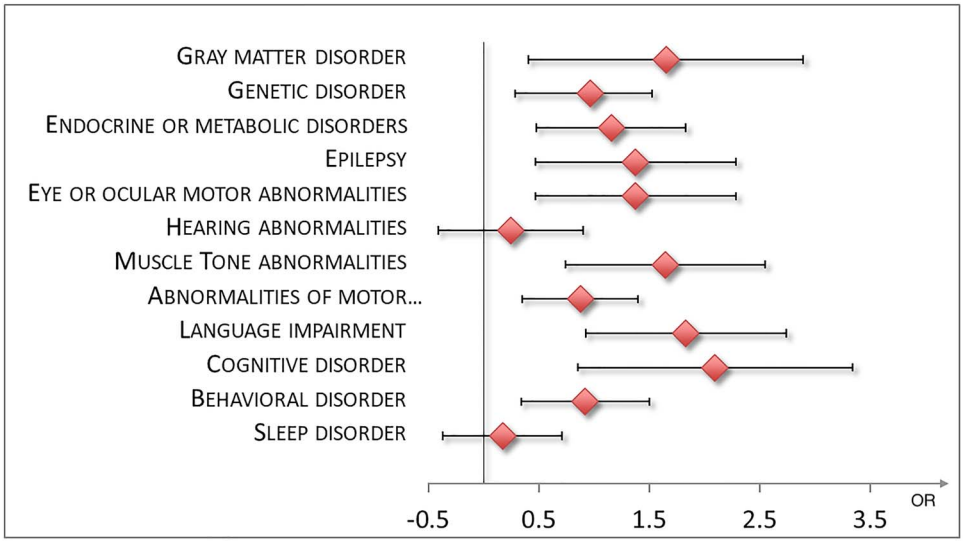

Figure 5. Forest plot of additional disorders (on the left) with the logarithmically scaled values of the odds ratios (red squares) and associated CIs (lateral tips of the squares) for the dCC patients and controls.

Table 6 Comparisons of quantitative brain measurements between dCC and control groups

Measurements	Reference group controls (*N*)	dCC group (*N*)	Mean of differences	CI	*t* value	*P* value
Age	34	34	0.002	(−0.008, 0.013)	0.446	0.658
Brain volume (mm^3)	34	34	75.792	(−8.754, 160.338)	1.824	0.077
Volume of cortical GM (normalized by TB)	34	34	−0.069	(−0.082, -0.056)	−0.107	$\mathbf{2.573\times10^{-12}}$
WM volume (normalized by TB)	34	34	0.023	(0.009, 0.037)	3.445	$\mathbf{1.574\times10^{-3}}$
GI_LH	34	34	0.232	(0.179, 0.285)	8.921	$\mathbf{2.608\times10^{-10}}$
GI_RH	34	34	0.244	(0.189, 0.300)	8.925	$\mathbf{2.581\times10^{-10}}$
Mean CT LH (mm)	32	32	−0.901	(−1.024, -0.778)	−0.149	$\mathbf{1.017\times10^{-15}}$
Mean CT RH (mm)	32	32	−0.902	(−1.014, -0.790)	−0.164	$\mathbf{7.365\times10^{-17}}$

Note: Significant *P* values are shown in bold. *N*, number of subjects. Results of paired *t*-tests were provided, and Bonferroni correction was applied. Confidence level: 95%.

Table 7 Comparisons of quantitative cortical DTI measurements between dCC and control groups

Measurements	Reference group controls (*N*)	dCC group (*N*)	Mean of differences	CI	*t* value	*P* value
Age	16	16	0.002	(−0.013, 0.017)	0.274	0.788
FA of the cerebral cortex	16	16	0.002	(−0.017, 0.021)	0.224	0.826
ADC of the cerebral cortex	16	16	-4.364×10^{-6}	(-5.991×10^{-5}, 5.119×10^{-5})	−0.167	0.869

Note: Results of paired *t*-tests were provided, and Bonferroni correction was applied. Confidence level: 95%.

The most frequently observed deficits in our study were language disorders, which were also the most extensively studied disorders in patients with dCC. The most common language impairments in our cohort were impairments in expressive language or a combination of expressive and receptive language difficulties. These results agree with the literature (Buchanan et al. 1980; Jeeves 1994) that reported frequent difficulties for patients with dCC to verbally express, for example, their emotional experiences (Buchanan et al. 1980). Furthermore, difficulties in the expressive language in dCC patients have often been observed as an "out of the place" conversations (Jeeves 1994). In addition to language difficulties, almost two-thirds of patients with dCC had developmental delay/cognitive deficits. Patients with dCC have usually an IQ within the normal range (Chiarello

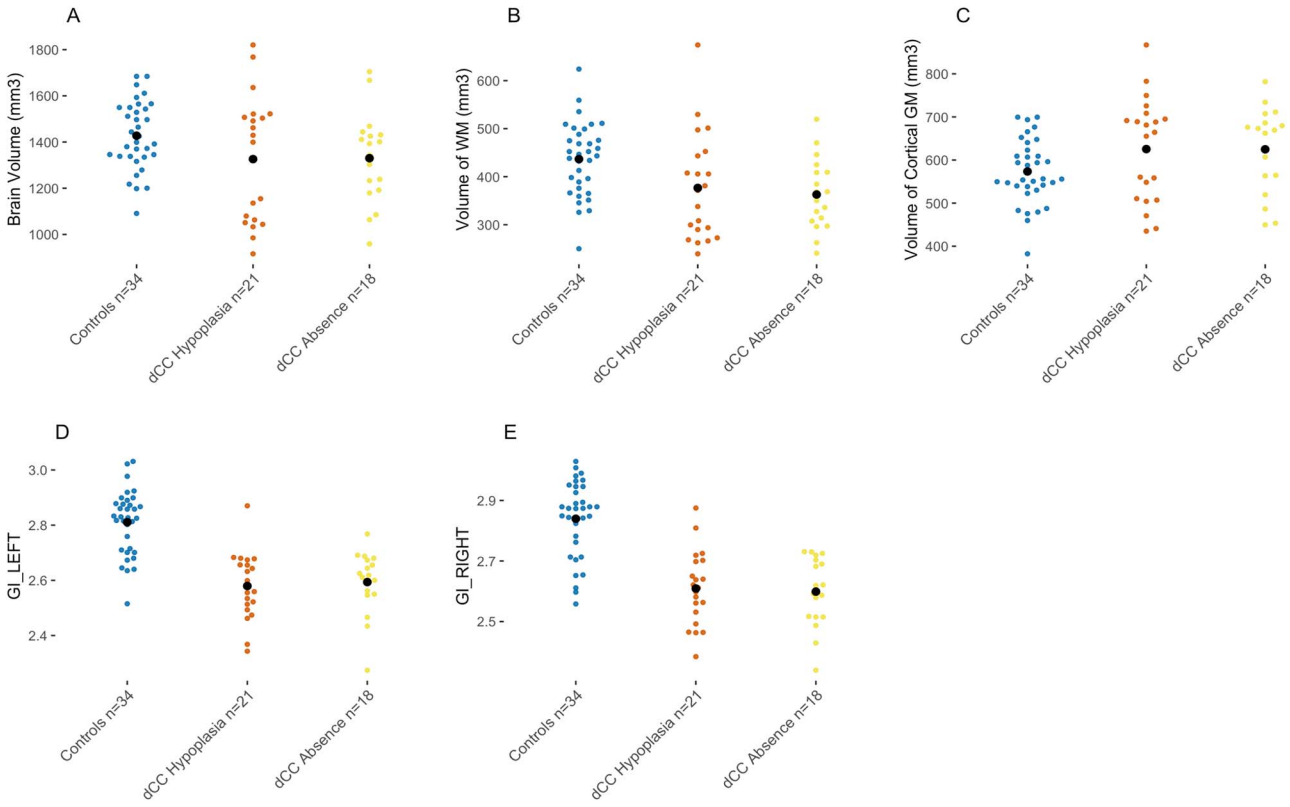

Figure 6. Scatterplots showing the comparison of mean brain volume (*A*), volume of the WM (*B*), mean cortical GM volume (*C*), and GI of the left (*D*) and right (*E*) hemisphere between the control group (blue) and dCC hypoplasia patients (orange), dCC absence patients (yellow). The black dots represent the means in each group.

1980). However, dCC patients frequently display problem-solving deficits (Fischer et al. 1992; Imamura et al. 1994), which might explain that the higher incidence of developmental delay also observed in our study. One of the interesting findings of our study was the presence of endocrine or metabolic disorders in almost half of the dCC patients. Hypothalamic diseases have been associated with abnormalities in the form of other midline structures, including the CC (Page et al. 1989).

Our findings suggest higher odds of discovering the presence of different clinical symptoms in patients with dCC compared to the controls. However, although these findings are in agreement with the findings reported in the literature, wide CIs within our study suggest that the presence and severity of the midline CC abnormality alone cannot explain the presence and various severity of these symptoms, although a larger cohort of dCC patients might be necessary in order to conclude on this.

Maturation of the Cerebral Cortex

The proper establishment of connections that carry sensory input from the environment (such as thalamo-cortical connections) is crucial for the normal microstructural maturation of the cerebral cortex. The maturation of the cerebral cortex is modulated by environmental inputs and involves the processes of synaptogenesis, synaptic pruning, and dendritic arborization (Rakic 1988; Bourgeois et al. 1989;Ball et al. 2013; Batalle et al. 2019). Our results showed that dCC patients have preserved microstructures of the cerebral cortex, as revealed by ADC and FA, measures often used to assess the level of dendritic arborization in the cerebral cortex (Batalle et al. 2019). Therefore, these results, together with the observations from past studies (Ball et al. 2013; Batalle et al. 2019), indicate that certain aspects of cortical maturation, indexed with ADC and FA, might be regulated by genes and environment and less by modulation of interhemispheric signal transfer. However, it is still possible that regional abnormalities of ADC and FA present in these patients, because in this study we have used only global measures of ADC and FA.

Our results revealed that in the absence global microstructural changes in the cerebral cortex, dCC patients had significantly smaller GIs and significantly thicker CT compared to controls (Table 6). Previous studies on an animal model of absent CC revealed a "thinning" of CT (Abreu-Villaça et al. 2002; Ribeiro–Carvalho et al. 2006) whereas a "thicker" CT in human patients with absent CC (Beaulé et al. 2015). The CT reduction in mice was explained by a possible effect on the cell death model during the developmental stage by callosal inputs (Ribeiro-Carvalho et al. 2006), while the greater CT in patients was hypothesized that some neuronal groups missing their targets may form nodules of cortical lines, and abnormal neuronal migration may form an atypical cortical organization (Guerrini et al. 2003; Guerrini and Marini 2006; Hyde et al. 2007; Beaulé et al. 2015).

Tarui et al. (2018) did not study the change in cortical surface or thickness in dCC fetuses during prenatal development, but they reported alterations in absolute sulcal positions and alterations in the spatial relationship between sulci in dCC fetuses. These alterations of the cortical surface landscape could be detected as early as the second trimester of gestation (Tarui et al. 2018). On the other hand, they reported that the traditional GI did not show significant differences in fetal dCC patients (Tarui et al. 2018; they called AgCC), whereas our results revealed a

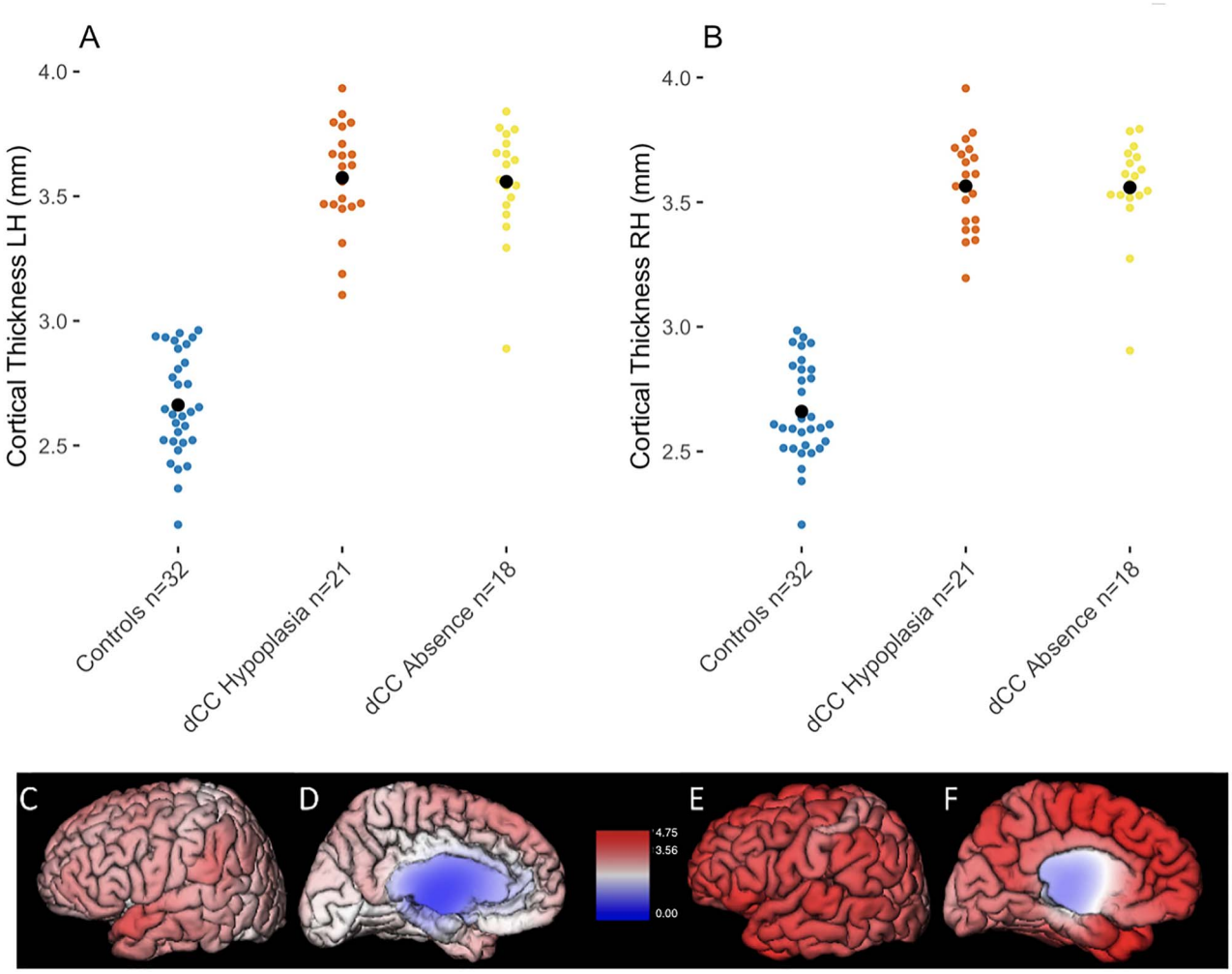

Figure 7. Scatter plots showing the comparison of mean CT of the LH (*A*) and mean CT of the RH (*B*) between the control group (blue) and dCC hypoplasia patients (orange), dCC absence patients (yellow). The black dots represent the means in each group. Regional CT maps of the LH in 10-year-old control subject (*C*, *D*) and 10-year-old dCC patient with hypoplastic CC (*E*, *F*). CT was color coded according to the map in the middle of the figure.

significant decrease in GI in dCC patients compared to controls in the postnatal population. Considering the age range included in these studies, the results from the two studies are not in conflict, and in fact, if the GI time courses presented by Tarui et al. (2018) were to continue to follow their given trajectories postnatally, it would corroborate the finding in this study that the GI is decreased in dCC versus neurotypical individuals.

Correlations between Brain MRI Findings and Clinical/Cognitive Characteristics

In the correlation analyses of brain MRI findings (both radiologically reported brain abnormalities [CC, GM, and brain size abnormalities] and quantitative measurements [TB volume, cortical GM volume, WM volume, GI in LH/RH, CT in LH/RH]) and clinical/cognitive characteristics were analyzed. As of our knowledge, our current study is the first that correlates both radiological brain anomalies and quantitative MRI measurements with clinical outcomes in dCC patients. Previous studies showed a significant positive correlation between WM volume and cognitive function (Gautam et al. 2015a; Taki et al. 2011; Walhovd and Fjell 2007). Interestingly, although in this study GM volume was increased in dCC and correlated with cognitive disorder, WM volume was decreased in dCC and not correlated with cognitive disorder. These results are suggestive of a potential compensation process in the GM (e.g., increased local within-GM connections) in response to the WM reduction.

In this study, RH CT was linked to language abnormalities. There were many studies on correlations between language functions and brain MRI measures, which were often complicated and had not achieved consensus. While quite a few studies commonly reported that language functions were associated with lateralization in the brain (Hécaen et al. 1981), the LH and RH contributions to language processing change throughout life (Olulade et al. 2020). However, there were a limited number of research studies that handled a wide age range like in our study (from 1.43 to 19.06 YO). Results from Ma et al. (2014) (from 7.7 to 16 YO) revealed that patients with dyslexia not only showed increased CT of the left fusiform gyrus compared to controls, but also showed increased CT in the right superior temporal gyrus, extending into the planum temporale. Paldino et al. (2016) studied the arcuate fasciculus (AF) in patients with malformations of

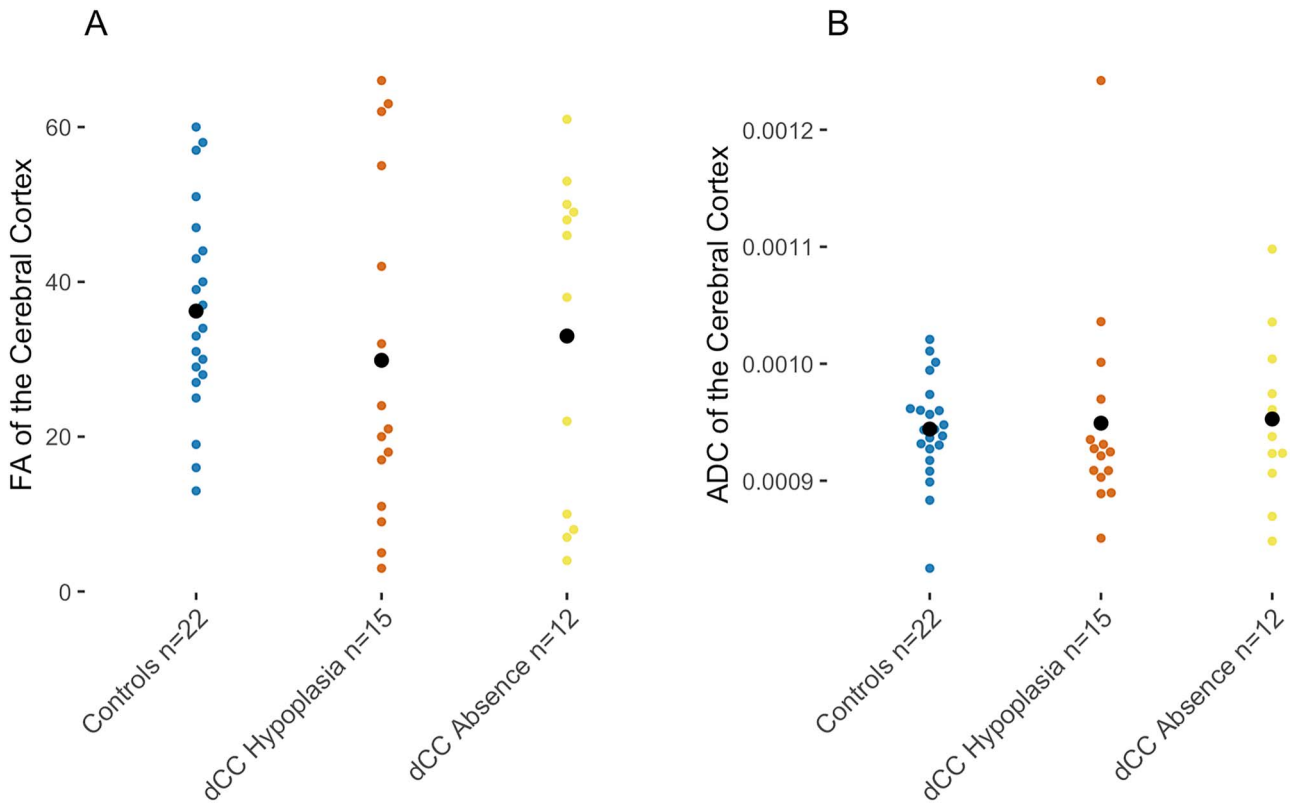

Figure 8. Scatter plots showing the comparison of mean cortical FA (A) and mean cortical ADC (B) between the control group (blue) and dCC hypoplasia patients (orange), dCC absence patients (yellow). The black dots represent the means in each group.

cortical development (from 3 to 18 YO) and reported that a non-identifiable left AF with diffusion MRI tractography was a strong marker of language dysfunctions, while the right AF was also important for oral language functions. In our past diffusion MRI tractography study on neurologically healthy subjects ranging from 0 to 28 YO, subsegments of the AF showed rightward asymmetry (Wilkinson et al. 2017). In this study, we were not able to perform our analyses by age because of the limited number of patients and controls in each age range. However, given the importance of age in language development, it would be crucial to study language development in dCC patients in the near future.

Previous studies supported the hypothesis that cortical gyrification was positively related to cognitive function during development. A study from (Chung et al. 2017) provided the evidence suggesting cortical gyrification could be relevant to general cognitive ability in healthy adulthood (12–25 YO). Results from Lamballais et al. (2020) suggested that gyrification varied with aging and cognition during and after midlife and that gyrification was a potential marker for age-related brain and cognitive decline beyond midlife. Similarly, greater cortical gyrification was shown to be associated with higher cognitive abilities in healthy midlife adulthood (Gautam et al. 2015b) and childhood/adolescence (White et al. 2010). There were also research studies focusing on local gyrification with diseases. For example, MacKinley et al. (2020) found that a deeper superior frontal sulcus predicted better cognitive scores among patients with schizophrenia (average 38.49 YO). Study from Wang et al. (2020) revealed that aberrant gyrification may underlie cognitive performance in premature children (8–12 YO). They found that the local GI in the precuneus and cingulate cortices were positively correlated with IQ scores in males with premutation (and in their controls), while negatively in females with premutation (not in their controls). Hedderich et al. (2019) provided evidence that both aberrant gyrification itself as well as its propagation across the cortex expressed aspects of impaired neurodevelopment after premature birth and led to reduced cognitive performance in adulthood (very preterm/very low birth weight: 27.5–28.3 YO, full term: 25.5–28.9 YO). In addition, Wallace et al. (2013) found greater gyrification in the left precuneus and bilateral posterior temporal/lateral occipital regions of adolescent and young adult males with ASD as compared to age- and IQ-matched typically developing males. They also found a robust positive correlation between vocabulary knowledge and gyrification in the left inferior parietal cortex in the typically developing group. However, little is known about how GI in LH and RH may differently affect cognitive functions. Our study fills this gap, indicating that the LH GI might have a more significant correlation with cognitive functions.

GM abnormalities and brain size abnormalities from radiological reviews were closely related to cortical GM volume and TB volume in quantitative MRI measurements respectively, however, several more significance were found in later analyses (Table 4) than former analyses (Table 3). Besides the significance of correlations shown in Table 3, for GM volume, there were three more statistically significant correlations (metabolic or endocrine disorder, cognitive disorder, and behavioral disorder),

and for TB volume, there were two more statistically significant correlations (muscle tone abnormality and metabolic or endocrine disorder), as shown in Table 4. This might be because that the three brain abnormalities were reported categorically with several different abnormalities such as GM ectopia/injury or brain size microcephaly/holoprosencephaly, while the quantitative MRI measurements were reported numerically with only the volumes of GM and TB. Therefore, the effects of numerical changes on clinical/cognitive characteristics could be better detected in multiple logistic regression models of quantitative MRI measurements than in categorically reported abnormalities.

Previous studies suggested CC atrophy may be associated with cognitive and motor deficits (Hampel et al. 1998; Jokinen et al. 2007; Ryberg et al. 2008). Our study also found significant relationship between CC abnormalities and motor skills/movement abnormalities, but not between CC abnormalities and cognitive disorders. Subjects who did not have CC abnormalities all did not have cognitive disorders ("complete separation", a phenomenon in statistics), which likely caused the maximum likelihood estimation of coefficients in logistic regression to diverge, which was represented as the large standard error (Albert and Anderson 1984; McCullough and Vinod 2003) in Table 3. Probably because of this "separation" of the data, we did not find significant correlation with cognitive disorder.

Limitations and Future Research

Although we did not visually observe registration errors both in patients and controls for the data we used, and Supplementary Fig. S1 nicely showed an example of such registration, it is still possible that there was slight registration errors that might be larger in patients.

There were also limitations of our statistical tests. In the results shown in Table 4, every multiple logistic regression model was generated based on 71 samples (32 dCC and 39 controls). These 71 samples were mostly sex-/age-matched in dCC patients and controls, but they were not matched in every symptom; that is, the number of people "having" and "not having" each symptom were not the same. Many samples in the dCC group had some symptoms; however, there were also many samples with dCC without having symptoms. That was likely the reason why results in Table 4 were not identically consistent with results in Table 6, for example, TB volume can affect some symptoms, but TB volume was not statistically significantly different in dCC patients and controls.

Normally, the results might have highly affected by retrospective data collection. However, BCH conducts mostly standardized MRI scanning for routine imaging as well. So that, this allows us to obtain quality retrospective MRI data. Our dataset, while having standardization advantages over most clinical centers (BCH installed a suite of 3T Skyra Siemens MRI scanners in 2007, while most clinical centers have a variety of different MRI scanners), we have standardization disadvantages relative to typical prospective studies (in which all T1 volumetric examinations are normally acquired with an identical MRI pulse sequence). This inevitably introduces additional variability/error in our measurements and when designing our analytic strategies for assessing our data, we felt it was important to be particularly cautious when presenting an effect that appears to be associated with the presentation of dCC clinically. Therefore, the most stringent accepted method was used to reduce the false discovery rate and thus limited the likelihood that our analysis reports findings that will not be confirmed in future studies. Type II errors were of far less concern to us, as this was akin to accidentally declaring no effect associated with dCC when a real effect was present. Our analysis was most concerned with assessing the largest effects, and we recognized that a heterogeneous clinical population was not likely to be the best method available for assessing the existence of small effect sizes, thus our reduced concern for type II errors, which in turn led to our decision to employ the particularly stringent Bonferroni correction in this analysis.

Behavioral tests were not performed for our control patients because of the retrospective nature of this study. A further prospective study may address the same behavioral and clinical evaluations across groups.

Conclusion

Patients with corpus callosal abnormalities had normal TB volume and overall tissue microstructures with potentially deteriorated mechanisms to expand/fold the brain, indicated by GI. Our brain MRI-based measures successfully revealed differential links to many symptoms, and our results suggest that the LH GI abnormality can be a unique predictor for the patients with corpus callosal abnormalities, which was uniquely associated with the patients' symptom (cognitive disorders).

Supplementary Material

Supplementary material can be found at *Cerebral Cortex* online.

Funding

This research study was supported by the National Institute of Neurological Disorders and Stroke (R01NS109475, R03NS091587 to E.T.), the National Institute of Mental Health (R21MH118739 to E.T.), and the Eunice Kennedy Shriver National Institute of Child Health and Human Development (R01HD078561, R21HD098606 to E.T.).

Notes

Dr Henry Feldman (BCH) provided advice on statistical analyses, and Ms Briana Valli (BCH) provided editorial assistance. Claude Lepage (McGill Centre for Integrative Neuroscience/Montreal Neurological Institute, McGill University, Canada) helped with MRI data processing.

Conflict of Interest: None declared.

References

Abreu-Villaça Y, Silva WC, Manhães AC, Schmidt SL. 2002. The effect of corpus callosum agenesis on neocortical thickness and neuronal density of BALB/cCF mice. *Brain Res Bull*. 58(4):411–416.

Albert A, Anderson JA. 1984. On the existence of maximum likelihood estimates in logistic regression models. *Biometrika*. 71(1):1–10.

Badaruddin DH, Andrews GL, Bölte S, Schilmoeller KJ, Schilmoeller G, Paul LK, Brown WS. 2007. Social and behavioral problems of children with agenesis of the corpus callosum. *Child Psychiatry Hum Dev*. 38(4):287–302.

Ball G, Srinivasan L, Aljabar P, Counsell SJ, Durighel G, Hajnal JV, Rutherford MA, Edwards AD. 2013. Development of cortical microstructure in the preterm human brain. *Proc Natl Acad Sci U S A*. 110(23):9541–9546.

Batalle D, O'Muircheartaigh J, Makropoulos A, Kelly CJ, Dimitrova R, Hughes EJ, Hajnal JV, Zhang H, Alexander DC, Edwards AD *et al*. 2019. Different patterns of cortical maturation before and after 38 weeks gestational age demonstrated by diffusion MRI in vivo. *Neuroimage*. 185:764–775.

Beaulé V, Tremblay S, Lafleur LP, Tremblay S, Lassonde M, Lepage JF, Théoret H. 2015. Cortical thickness in adults with agenesis of the corpus callosum. *Neuropsychologia*. 77: 359–365.

Bénézit A, Hertz-Pannier L, Dehaene-Lambertz G, Monzalvo K, Germanaud D, Duclap D, Guevara P, Mangin J-F, Poupon C, Moutard M-L. 2015. Organising white matter in a brain without corpus callosum fibres. *Cortex*. 63:155–171.

Boucher M, Whitesides S, Evans A. 2009. Depth potential function for folding pattern representation, registration and analysis. *Med Image Anal*. 13(2):203–214.

Bourgeois JP, Jastreboff PJ, Rakic P. 1989. Synaptogenesis in visual cortex of normal and preterm monkeys: evidence for intrinsic regulation of synaptic overproduction. *Proc Natl Acad Sci U S A*. 86(11):4297–4301.

Boyd EH, Pandya DN, Bignall KE. 1971. Homotopic and nonhomotopic interhemispheric cortical projections in the squirrel monkey. *Exp Neurol*. 32(2):256–274.

Buchanan DC, Waterhouse GJ, West SC Jr. 1980. A proposed neurophysiological basis of alexithymia. *Psychother Psychosom*. 34(4):248–255.

Cauller LJ, Clancy B, Connors BW. 1998. Backward cortical projections to primary somatosensory cortex in rats extend long horizontal axons in layer I. *J Comp Neurol*. 390(2): 297–310.

Chiarello C. 1980. A house divided? Cognitive functioning with callosal agenesis. *Brain Lang*. 11(1):128–158.

Chung YS, Hyatt CJ, Stevens MC. 2017. Adolescent maturation of the relationship between cortical gyrification and cognitive ability. *NeuroImage*. 158:319–331.

Edwards TJ, Sherr EH, Barkovich AJ, Richards LJ. 2014. Clinical, genetic and imaging findings identify new causes for corpus callosum development syndromes. *Brain*. 137(Pt 6):1579–1613.

Fenlon LR, Richards LJ. 2015. Contralateral targeting of the corpus callosum in normal and pathological brain function. *Trends Neurosci*. 38(5):264–272.

Fischer M, Ryan SB, Dobyns WB. 1992. Mechanisms of interhemispheric transfer and patterns of cognitive function in acallosal patients of normal intelligence. *Arch Neurol*. 49(3):271–277.

Fonov VS, Evans AC, McKinstry RC, Almli C, Collins D. 2009. Unbiased nonlinear average age-appropriate brain templates from birth to adulthood. *Neuroimage*. 47:S102.

Gautam P, Anstey KJ, Wen W, Sachdev PS, Cherbuin N. 2015a. Cortical gyrification and its relationships with cortical volume, cortical thickness, and cognitive performance in healthy mid-life adults. *Behav Brain Res*. 287:331–339.

Gautam P, Lebel C, Narr KL, Mattson SN, May PA, Adnams CM, Riley EP, Jones KL, Kan EC, Sowell ER. 2015b. Volume changes and brain-behavior relationships in white matter and subcortical gray matter in children with prenatal alcohol exposure. *Hum Brain Mapp*. 36:2318–2329.

Gobius I, Richards L. 2011. Creating connections in the developing brain: Mechanisms regulating corpus collosum development. M.M. McCarthy (Ed.), Colloquium Series in the Developing Brain, Morgan & Claypool Lifesciences, New Jersey, pp. 1–48.

Goodyear PW, Bannister CM, Russell S, Rimmer S. 2001. Outcome in prenatally diagnosed fetal agenesis of the corpus callosum. *Fetal Diagn Ther*. 16(3):139–145.

Guerrini R, Marini C. 2006. Genetic malformations of cortical development. *Exp Brain Res*. 173(2):322–333.

Guerrini R, Sicca F, Parmeggiani L. 2003. Epilepsy and malformations of the cerebral cortex. *Epileptic Disord*. 5(Suppl 2):S9–S26.

Hampel H, Teipel SJ, Alexander GE, Horwitz B, Teichberg D, Schapiro MB, Rapoport SI. 1998. Corpus callosum atrophy is a possible indicator of region- and cell type-specific neuronal degeneration in Alzheimer disease: a magnetic resonance imaging analysis. *Arch Neurol*. 55(2):193–198.

Hécaen H, De Agostini M, Monzon-Montes A. 1981. Cerebral organization in left-handers. *Brain Lang*. 12(2):261–284.

Hedderich DM, Bäuml JG, Berndt MT, Menegaux A, Scheef L, Daamen M, Zimmer C, Bartmann P, Boecker H, Wolke D *et al*. 2019. Aberrant gyrification contributes to the link between gestational age and adult IQ after premature birth. *Brain*. 142(5):1255–1269.

Heimer G, Marek-Yagel D, Eyal E, Barel O, Oz Levi D, Hoffmann C, Ruzzo EK, Ganelin-Cohen E, Lancet D, Pras E *et al*. 2015. SLC1A4 mutations cause a novel disorder of intellectual disability, progressive microcephaly, spasticity and thin corpus callosum. *Clin Genet*. 88(4):327–335.

Hetts SW, Sherr EH, Chao S, Gobuty S, Barkovich AJ. 2006. Anomalies of the corpus callosum: an MR analysis of the phenotypic spectrum of associated malformations. *AJR Am J Roentgenol*. 187(5):1343–1348.

Hyde KL, Lerch JP, Zatorre RJ, Griffiths TD, Evans AC, Peretz I. 2007. Cortical thickness in congenital amusia: when less is better than more. *J Neurosci*. 27(47):13028–13032.

Imamura T, Yamadori A, Shiga Y, Sahara M, Abiko H. 1994. Is disturbed transfer of learning in callosal agenesis due to a disconnection syndrome? *Behav Neurol*. 7(2):43–48.

Jeeves MA. 1994. *Callosal agenesis—a natural split-brain overview*. In: Lassonde M, Jeeves MA, editors. Callosal Agenesis. Advances in Behavioral Biology, vol 42. Boston, MA: Springer, pp. 285–299.

Jokinen H, Ryberg C, Kalska H, Ylikoski R, Rostrup E, Stegmann MB, Waldemar G, Madureira S, Ferro JM, van Straaten ECW *et al*. 2007. Corpus callosum atrophy is associated with mental slowing and executive deficits in subjects with age-related white matter hyperintensities: the LADIS Study. *J Neurol Neurosurg Psychiatry*. 78(5): 491–496.

Kim JS, Singh V, Lee JK, Lerch J, Ad-Dab'bagh Y, MacDonald D, Lee JM, Kim SI, Evans AC. 2005. Automated 3-D extraction and evaluation of the inner and outer cortical surfaces using a Laplacian map and partial volume effect classification. *Neuroimage*. 27(1):210–221.

Kretz R, Rager G. 1990. Reciprocal heterotopic callosal connections between the two striate areas in Tupaia. *Exp Brain Res*. 82(2):271–278.

Kroner BL, Preiss LR, Ardini M-A, Gaillard WD. 2008. New incidence, prevalence, and survival of Aicardi syndrome from 408 cases. *J Child Neurol*. 23(5):531–535.

Lamballais S, Vinke EJ, Vernooij MW, Ikram MA, Muetzel RL. 2020. Cortical gyrification in relation to age and cognition in older adults. *Neuroimage*. 212:116637.

Lyttelton O, Boucher M, Robbins S, Evans A. 2007. An unbiased iterative group registration template for cortical surface analysis. *Neuroimage*. 34(4):1535–1544.

Ma Y, Koyama MS, Milham MP, Castellanos FX, Quinn BT, Pardoe H, Wang X, Kuzniecky R, Devinsky O, Thesen T et al. 2014. Cortical thickness abnormalities associated with dyslexia. independent of remediation status. Neuroimage Clin. 7:177–186.

MacDonald D, Kabani N, Avis D, Evans AC. 2000. Automated 3-D extraction of inner and outer surfaces of cerebral cortex from MRI. *Neuroimage*. 12(3):340–356.

MacKinley ML, Sabesan P, Palaniyappan L. 2020. Deviant cortical sulcation related to schizophrenia and cognitive deficits in the second trimester. *Transl Neurosci*. 11(1):236–240.

Mitchell BD, Macklis JD. 2005. Large-scale maintenance of dual projections by callosal and frontal cortical projection neurons in adult mice. *J Comp Neurol*. 482(1):17–32.

McCullough BD, Vinod HD. 2003. Verifying the solution from a nonlinear solver: a case study. *Am Econ Rev*. 93(3):873–892.

Mooshagian E, Iacoboni M, Zaidel E. 2009. Spatial attention and interhemispheric visuomotor integration in the absence of the corpus callosum. *Neuropsychologia*. 47(3): 933–937.

Moutard ML, Kieffer V, Feingold J, Kieffer F, Lewin F, Adamsbaum C, Gélot A, Campistol i Plana J, van Bogaert P, André M *et al*. 2003. Agenesis of corpus callosum: prenatal diagnosis and prognosis. *Childs Nerv Syst*. 19(7-8):471–476.

Olulade OA, Seydell-Greenwald A, Chambers CE, Turkeltaub PE, Dromerick AW, Berl MM, Gaillard WD, Newport EL. 2020. The neural basis of language development: Changes in lateralization over age. *PNAS U S A*. 117(38):23477–23483.

Page SR, Nussey SS, Jenkins JS, Wilson SG, Johnson DA. 1989. Hypothalamic disease in association with dysgenesis of the corpus callosum. *Postgrad Med J*. 65(761): 163–167.

Paldino MJ, Hedges K, Golriz F. 2016. The arcuate fasciculus and language development in a cohort of pediatric patients with malformations of cortical development. *Am J Neuroradiol*. 37(1):169–175.

Palmer EE, Mowat D. 2014. Agenesis of the corpus callosum: a clinical approach to diagnosis. *Am J Med Genet C Semin Med Genet*. 166c(2):184–197.

Paul LK, Brown WS, Adolphs R, Tyszka JM, Richards LJ, Mukherjee P, Sherr EH. 2007. Agenesis of the corpus callosum: genetic, developmental and functional aspects of connectivity. *Nat Rev Neurosci*. 8(4):287–299.

Petreanu L, Huber D, Sobczyk A, Svoboda K. 2007. Channelrhodopsin-2-assisted circuit mapping of long-range callosal projections. *Nat Neurosci*. 10(5):663–668.

Pienaar R, Rannou N, Bernal J, Hahn D, Grant PE. 2015. ChRIS – A web-based neuroimaging and informatics system for collecting, organizing, processing, visualizing and sharing of medical data. *Conf Proc IEEE Eng Med Biol Soc*. 2015: 206–209.

Rakic P. 1988. Specification of cerebral cortical areas. *Science*. 241(4862):170–176.

Ribeiro-Carvalho A, Manhães AC, Abreu-Villaça Y, Filgueiras CC. 2006. Early callosal absence disrupts the establishment of normal neocortical structure in Swiss mice. *Int J Dev Neurosci*. 24(1):15–21.

Robbins SM. 2004. *Anatomical standardization of the human brain in euclidean 3-space and on the cortical 2-manifold*. (Doctoral Dissertation). School of Computer Science, McGill University, Montreal, Que., Canada.

Rotmensch S, Monteagudo A. 2020. Agenesis of the corpus callosum. *Am J Obstet Gynecol*. 223(6):B17–b22.

Ryberg C, Rostrup E, Sjöstrand K, Paulson OB, Barkhof F, Scheltens P, van Straaten ECW, Fazekas F, Schmidt R, Erkinjuntti T *et al*. 2008. White matter changes contribute to corpus callosum atrophy in the elderly: the LADIS study.. *Am J Neuroradiol*. 29(8):1498–1504.

Sauerwein HC, Lassonde MC, Cardu B, Geoffroy G. 1981. Interhemispheric integration of sensory and motor functions in agenesis of the corpus callosum. *Neuropsychologia*. 19(3):445–454.

Schell-Apacik CC, Wagner K, Bihler M, Ertl-Wagner B, Heinrich U, Klopocki E, Kalscheuer VM, Muenke M, von Voss H. 2008. Agenesis and dysgenesis of the corpus callosum: clinical, genetic and neuroimaging findings in a series of 41 patients. *Am J Med Genet A*. 146a(19):2501–11.

Schmahmann JD, Pandya DN, Wang R, Dai G, D'Arceuil HE, de Crespigny AJ, Wedeen VJ. 2007. Association fibre pathways of the brain: parallel observations from diffusion spectrum imaging and autoradiography. *Brain*. 130(Pt 3):630–653.

Sherif T, Rioux P, Rousseau M-E, Kassis N, Beck N, Adalat R, Das S, Glatard T, Evans AC. 2014. CBRAIN: a web-based, distributed computing platform for collaborative neuroimaging research. *Front Neuroinform*. 8:54–54.

Shevell MI. 2002. Clinical and diagnostic profile of agenesis of the corpus callosum. *J Child Neurol*. 17(12):895–899.

Sled JG, Zijdenbos AP, Evans AC. 1998. A nonparametric method for automatic correction of intensity nonuniformity in MRI data. *IEEE Trans Med Imaging*. 17(1):87–97.

Song JW, Mitchell PD, Kolasinski J, Ellen Grant P, Galaburda AM, Takahashi E. 2015. Asymmetry of white matter pathways in developing human brains. *Cereb Cortex (New York, NY: 1991)*. 25(9):2883–2893.

Takahashi E, Dai G, Wang R, Ohki K, Rosen GD, Galaburda AM, Grant PE, Wedeen VJ. 2010. Development of cerebral fiber pathways in cats revealed by diffusion spectrum imaging. *Neuroimage*. 49(2):1231–1240.

Takahashi E, Folkerth RD, Galaburda AM, Grant PE. 2011. Emerging cerebral connectivity in the human fetal brain: an MR tractography study. *Cereb Cortex*. 22(2):455–464.

Takahashi E, Folkerth RD, Galaburda AM, Grant PE. 2012. Emerging cerebral connectivity in the human fetal brain: an MR tractography study. *Cereb Cortex*. 22(2):455–464.

Takahashi E, Hayashi E, Schmahmann JD, Ellen Grant P. 2014. Development of cerebellar connectivity in human fetal brains revealed by high angular resolution diffusion tractography. *Neuroimage*. 96:326–333.

Taki Y, Kinomura S, Sato K, Goto R, Wu K, Kawashima R, Fukuda H. 2011. Correlation between gray/white matter volume and cognition in healthy elderly people. *Brain Cogn*. 75(2):170–176.

Tarui T, Madan N, Farhat N, Kitano R, Ceren Tanritanir A, Graham G, Gagoski B, Craig A, Rollins CK, Ortinau C *et al*. 2018. Disorganized patterns of sulcal position in fetal brains with agenesis of corpus callosum. *Cereb Cortex*. 28(9): 3192–3203.

Tohka J, Zijdenbos A, Evans A. 2004. Fast and robust parameter estimation for statistical partial volume models in brain MRI. *Neuroimage*. 23(1):84–97.

Tovar-Moll F, Moll J, de Oliveira-Souza R, Bramati I, Andreiuolo PA, Lent R. 2007. Neuroplasticity in human callosal dysgenesis: a diffusion tensor imaging study. *Cereb Cortex*. 17(3):531–541.

Vasung L, Charvet CJ, Shiohama T, Gagoski B, Levman J, Takahashi E. 2019. Ex vivo fetal brain MRI: recent advances, challenges, and future directions. *Neuroimage*. 195:23–37.

Vasung L, Yun HJ, Feldman HA, Grant PE, Im K. 2020. An atypical sulcal pattern in children with disorders of the corpus callosum and its relation to behavioral outcomes. *Cereb Cortex*. 30(9):4790–4799.

Veinante P, Deschenes M. 2003. Single-cell study of motor cortex projections to the barrel field in rats. *J Comp Neurol*. 464(1):98–103.

Walhovd KB, Fjell AM. 2007. White matter volume predicts reaction time instability. *Neuropsychologia*. 45(10):2277–2284.

Wallace GL, Robustelli B, Dankner N, Kenworthy L, Giedd JN, Martin A. 2013. Increased gyrification, but comparable surface area in adolescents with autism spectrum disorders. *Brain : a journal of neurology*. 136(Pt 6):1956–1967.

Wang JY, Danial M, Soleymanzadeh C, Kim B, Xia Y, Kim K, Tassone F, Hagerman RJ, Rivera SM. 2020. Cortical gyrification and its relationships with molecular measures and cognition in children with the FMR1 premutation. *Sci Rep*. 10(1):16059.

Wedeen VJ, Wang RP, Schmahmann JD, Benner T, Tseng WY, Dai G, Pandya DN, Hagmann P, D'Arceuil H, de Crespigny AJ. 2008. Diffusion spectrum magnetic resonance imaging (DSI) tractography of crossing fibers. *Neuroimage*. 41(4):1267–1277.

White T, Su S, Schmidt M, Kao C-Y, Sapiro G. 2010. The development of gyrification in childhood and adolescence. *Brain Cogn*. 72(1):36–45.

Wilkinson M, Lim AR, Cohen AH, Galaburda AM, Takahashi E. 2017. Detection and growth pattern of arcuate fasciculus from newborn to adult. *Front. Neurosci*. 11:389.

Yorke CH Jr, Caviness VS Jr. 1975. Interhemispheric neocortical connections of the corpus callosum in the normal mouse: a study based on anterograde and retrograde methods. *J Comp Neurol*. 164(2):233–245.

Yuan J, Song X, Kuan E, Wang S, Zuo L, Ongur D, Hu W, Du F. 2020. The structural basis for interhemispheric functional connectivity: evidence from individuals with agenesis of the corpus callosum. *NeuroImage: Clinical*. 28:102425.

Zijdenbos A, Forghani R, Evans A. 1998. Automatic quantification of MS lesions in 3D MRI brain data sets: validation of INSECT. In: Wells WM, Colchester A, Delp S, editors. *Medical Image Computing and Computer-Assisted Intervention — MICCAI'98*. MICCAI 1998. Lecture Notes in Computer Science, vol 1496. Berlin, Heidelberg: Springer. https://doi.org/10.1007/BFb0056229.